Structure and Toughness of Polyethersulfone (PESU)-Modified Anhydride-Cured Tetrafunctional Epoxy Resin: Effect of PESU Molecular Mass

S. Grishchuk,[1] O. Gryshchuk,[1] M. Weber,[2] J. Karger-Kocsis[3,4]

[1]*Institut für Verbundwerkstoffe GmbH (Institute for Composite Materials), Kaiserslautern University of Technology, D-67663 Kaiserslautern, Germany*
[2]*BASF SE, GKT/B—B1 D-67056 Ludwigshafen, Germany*
[3]*Department of Polymer Engineering, Faculty of Mechanical Engineering, Budapest University of Technology and Economics, H-1111 Budapest, Hungary*
[4]*Department of Polymer Technology, Faculty of Engineering and Built Environment, Tshwane University of Technology, Pretoria 0001, Republic of South Africa*

Received 11 February 2011; accepted 29 March 2011
DOI 10.1002/app.34610
Published online 12 August 2011 in Wiley Online Library (wileyonlinelibrary.com).

ABSTRACT: A tetrafunctional, anhydride hardened epoxy resin (EP) was modified with polyethersulfones (PESU) of different molecular mass (MM) without using additional solvent in 10 wt %. The morphology, thermal, and fracture mechanical properties of the EP/PESU systems were determined. PESU was present as dispersed phase in the EP matrix. The final morphology of EP/PESU depended on MM of PESU. PESU of low and medium MM formed submicron scale spherical droplets, whereas PESU of high MM was present in micron scale inclusions of complex (sea-island) structure. With increasing MM of PESU, the fracture mechanical properties, and especially the fracture energy, were increased. This was traced to differences in the morphology (dispersion of PESU) of the EP/PESU systems triggering different failure mechanisms. The onset of thermal degradation was slightly reduced, whereas the char yield enhanced by PESU modification compared with the reference EP. © 2011 Wiley Periodicals, Inc. J Appl Polym Sci 123: 1193–1200, 2012

Key words: thermosets; toughness; structure–property relationships; morphology; fracture

INTRODUCTION

Epoxy (EP) resins are widely used in a broad range of applications, especially in the aerospace, construction, electronic/electric, and automotive industries. This is mostly due to their easy processing, outstanding mechanical properties, thermal and solvent resistances. EP resins are preferred matrices of advanced composites in different structural applications. EP resins are inherently brittle materials due their high crosslink densities guaranteeing high glass transition temperature (T_g). This note holds especially for aerospace grade EP systems. The lack of toughness of EPs hampers their use and forced researchers to work on their efficient toughening. The common aspect of the toughening strategies is to add or create a second phase which—via the related morphology—triggers various energy absorbing mechanisms during fracture. The modifiers used are both of inorganic and organic origin. Organic modifiers, whether soluble or insoluble in the EP components, are mostly low molecular mass (MM) oligomers and polymers (e.g., liquid rubbers, hyperbranched polymers; MM $<$ 100 kDa), which usually have epoxy-reactive functional groups. Albeit they work as suitable tougheners, their incorporation in EPs is accompanied with undesirable changes in the mechanical (reduced stiffness and strength) and thermal properties (reduced T_g). To avoid this disadvantage, a large body of work has been addressed already the toughening of EP systems with amorphous or semicrystalline thermoplastics. Note that in this case, the toughness improvement is not associated with pronounced reductions in the basic mechanical and thermal properties. Great variety of thermoplastic polymers has been tried to modify EP resins, such as polymethyl methacrylate,[1] linear polyesters and copolyesters,[2,3] polyethylene oxide,[4] polycaprolactone,[5] polyoxymethylene,[6] polyamide,[7] styrene copolymers,[8] and polyphenylene oxide.[9] However, the research interest became focused on engineering thermoplastics (mostly amorphous ones)

Correspondence to: J. Karger-Kocsis (karger@pt.bme.hu).
Contract grant sponsor: Hungarian Scientific Research Fund; contract grant number: OTKA-NK 83421.
Contract grant sponsor: "Vulcan" of the European Union; contract grant number: AST5-CT-2006-031011.
Contract grant sponsors: German Science Fund (DFG); Advanced Manufacturing Technology Strategy program of DST (South Africa).

TABLE I
Main Characteristics of PESU Samples Used for Modification

Sample	PESU-L	PESU-M	PESU-H
Viscosity number (reduced viscosity) (mL/g)	27.1	33.5	45.1
—OH end group content (wt %)	0.54	0.36	0.22
Mean number-average MM, M_n (g/mol)	8800	12,500	16,800
Mean weight-average MM, M_w (g/mol)	16,300	27,600	39,000
T_g (DSC) (°C)	219	222	227

The viscosity number of the PESU-samples was determined using an Ubelohde-type viscosimeter at 25°C. The concentration of the polymer solution was 1 wt % in *N*-methylpyrrolidone. The viscosity number (reduced viscosity) is a guideline for the MM. The —OH end group content was determined by potentiometric titration in DMF-solution with 0.1 molar tetrabutylammoniumhydroxide solution. The molecular masses (M_w, M_n) were determined by GPC-measurements with dimethylacetamide/0.5 wt % LiBr as solvent. For calibration, PMMA-standards were used. The flow rate was 1 mL/min.

L, M, and H—low, medium, and high MM versions of PESU.

including polyaryl ether ketones,[10,11] polyetherimide,[12–16] polysulfones,[17–20] and especially polyethersulfone (PESU) derivatives.[21–35] An excellent review on thermoplastic-modified EPs was compiled by Hodgkin et al. in 1998.[23] To facilitate the dissolution of thermoplastics in the EP, additional solvents were often used. For PESU, usually methylene chloride serves as solvent.[21,24,30] Although this solvent-assisted modification is highly efficient, it is not environmental benign and thus it should be avoided. It was, however, reported that PESU can be dissolved directly in EP resins.[36–40] In this study, PESU was dissolved in liquid anhydride hardener.

It was early recognized that the morphology of the modified resin controls the fracture properties. On the other hand, the final morphology (particulate, cocontinuous, phase inverted) depends on material characteristics (e.g., solubility affected by MM and functionality), amount of the thermoplastic modifier, and especially on the curing conditions. Note that the thermoplastic-based "second phase" appears due to phase separation which takes place during curing. This is the reason why many works were devoted to the phase separation (segregation) process, also in case of EP/PESU systems.[28,29,32,34] It was also established that additional inorganic fillers (platy or fibrillar types) affect the phase separation[33,41,42] and thus represent further tools for the morphology control. It is obvious that the phase separation process in thermoplastic-modified EPs depends on the molecular mass (MM) of the thermoplastic toughener. This issue was less addressed in the past as researches mostly used commercially available thermoplastics. Nonetheless, in their review, Hodgkin et al.[23] concluded that the toughness of thermoplastic-modified EP increases with increasing MM of the toughener. The upper MM threshold depends upon requirements of the practical use because the viscosity of the EP strongly increases with the thermoplastic modification.

Accordingly, this work was aimed at studying the effects of MM of PESU, terminated with phenolic hydroxyl groups, on the fracture properties of an aerospace grade tetrafunctional EP hardened by anhydride. PESU has been dissolved in the anhydride hardener without the use of any solvent and mixed with the EP resin before curing. The morphology of the toughened EPs was determined by inspecting the fracture surface of the specimens, used to determine the fracture mechanical parameters (fracture toughness and energy), using the scanning electron microscope (SEM).

EXPERIMENTAL

Materials

Tetrafunctional EP (tetraglycidyl diaminodiphenylmethane, TGDDM) resin (Araldite®MY 721) was purchased from Huntsman Advanced Materials, Basel, Switzerland. The characteristics of this EP are as follows: epoxy equivalent mass = 109–116 g/eq, viscosity 3–6 Pa s at 50°C, and density 1.21 g/mL at 25°C.

As hardener methyl-tetrahydrophthalic anhydride (MTHPA; Aradur®HY 917) from Ciba Specialty Chemicals Corp. (Lampertheim, Germany) was selected. The characteristics of MTHPA are as follows: MM = 167 g/mol, anhydride content ≥97%, viscosity 50–100 mPa s at 25°C, and density 1.15–1.25 g/mL at 25°C.

1-Methylimidazol (DY 070; Huntsman Advanced Materials, Basel, Switzerland) was used as accelerator. Its characteristics are as follows: MM = 82 g/mol,

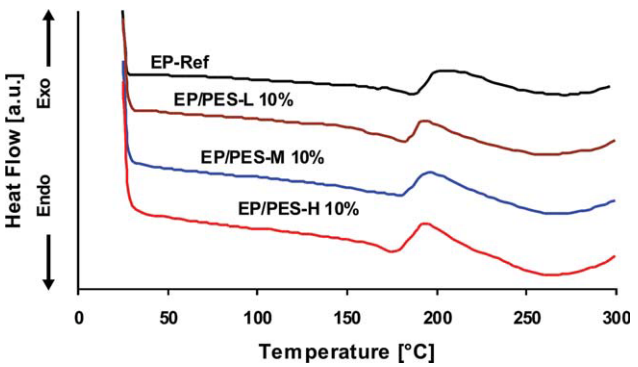

Figure 1 DSC traces of the EP and EP/PESU systems containing PESU of various MM in 10 wt %. [Color figure can be viewed in the online issue, which is available at wileyonlinelibrary.com.]

TABLE II
T_g (Derived from DSC and DMTA Measurements), Fracture Mechanical (K_c, G_c), and TGA Data for the EP and EP/PESU Systems Studied

Material	T_g(DSC), °C	T_g(DMA), °C	K_c (MPa m^{0,5})	G_c (J/m^2)	$K_{c,rel}$ (%)	$G_{c,rel}$ (%)	$T_{5\%}$ (°C)	Char yield at $T = 600$°C (%)
EP	180	213	0.62 ± 0.05	151 ± 21	100 ± 8	100 ± 14	332	9.5
EP/PESU-L 10%	170	197	0.61 ± 0.06	185 ± 13	99 ± 9	122 ± 7	295	13.9
EP/PESU-M 10%	169	204	0.62 ± 0.07	180 ± 30	101 ± 11	119 ± 17	330	11.9
EP/PESU-H 10%	168	202	0.90 ± 0.06	369 ± 45	146 ± 6	244 ±12	320	14.5

$K_{c,rel}$ (%) and $G_{c,rel}$ (%) indicate for the relative improvements in these fracture mechanical parameters.

viscosity ≤ 50 mPa s at 25°C; density 0.95–1.05 g/mL at 25°C.

The OH-terminated PESU materials with varying MM were experimental Ultrason® PESU products of BASF (Ludwigshafen, Germany). The main characteristics of the PESU samples, along with their coding are presented in Table I.

Preparation

As mentioned before, the influence of MM of PESU on the fracture mechanical properties of EP was investigated on systems containing 10 wt % of modifiers. The EP/PESU systems were produced as described below. PESU was mixed with the anhydride component at 80°C and kept for 24 h to achieve complete dissolution. The dissolved PESU markedly increased the viscosity of the anhydride component. Then, EP resin was added and mixed 10 min at 200 revolutions per minute (rpm). The mixture was degassed *in vacuo*. Then, the activator was added and mixed for 3 min at 200 rpm, degassed again, and poured in open molds fabricated from polytetrafluoro ethylene. Plates (100 × 10 × 4 mm^3, length × width × thickness) and compact tension (CT) specimens (35 × 35 × 4 mm^3, length × width × thickness) were produced in the cavities of the mold. All systems were cured for 4 h at 105°C with following postcuring at 160°C for 4 h. The molds were then cooled to ambient temperature over night and the specimens removed.

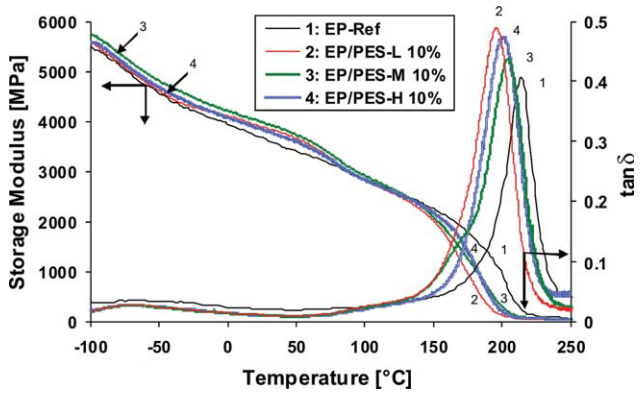

Figure 2 E' and tan δ as a function of T for EP and EP/PESU (10 wt %) containing PESU of low (L), medium (M), and high (H) MM. [Color figure can be viewed in the online issue, which is available at wileyonlinelibrary.com.]

Testing

The phase structure of the cured samples was studied by dynamic-mechanical thermal analysis (DMTA). DMTA traces (storage modulus, E'; and the mechanical loss factor, tan δ; vs. temperature) were determined by a DMA Q800 device of TA Instruments (New Castle, DE) on rectangular specimens (60 × 10 × 3 mm^3; length × width × thickness) in 3-point bending configuration (span length: 50 mm) at 10 Hz with an oscillation amplitude of 25 μm. The scan rate in the selected temperature range ($T = -100 \cdots +250$°C) was 1°C/min. The T_g was read as the peak temperature of the α-relaxation transition in the tan δ versus temperature curve of the related system.

Additionally, DSC traces were recorded by a DSC821 device of Mettler Toledo (Gießen, Germany) at 10°C/min heating rate in the temperature range of 25 to 300°C in nitrogen atmosphere. T_g was read at the mid point of the glass transition step.

The resins were subjected to thermogravimetric analysis (TGA) in a DTG-60 device of Shimadzu Deutschland GmbH (Duisburg, Germany). The TGA experiments were conducted under nitrogen atmosphere in the temperature range $T = +25$°C$\cdots$ +600°C with heating rate 10°C/min.

Fracture energy (G_c) and fracture toughness (K_c) were determined on CT specimens according to ISO 13586-1 standard. The CT specimens were initially notched by sawing. Their notch root was sharpened by a fresh razor blade before their tensile loading (mode I) at room temperature on a Zwick 1445 machine (Zwick GmbH, Ulm, Germany) with a crosshead speed of $v = 1$ mm/min. Surfaces of the broken CT specimens were inspected in a scanning electron microscope (SEM, JSM-5400 of Jeol, Tokyo, Japan). To avoid electric charging, the fracture surface was sputter coated with an Au/Pd alloy.

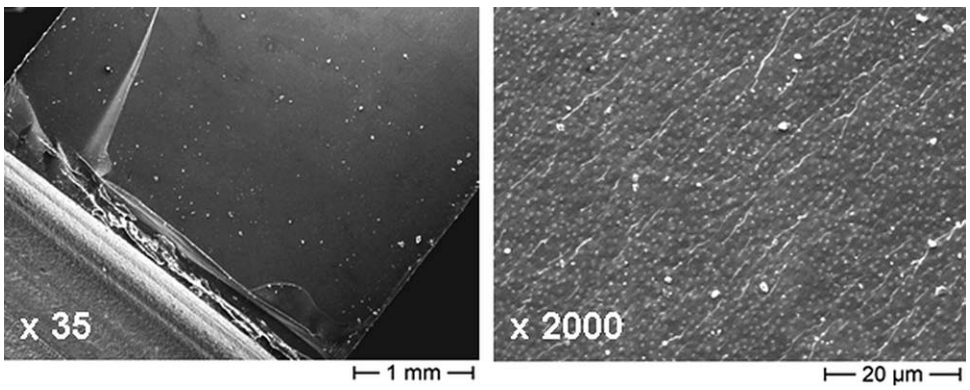

Figure 3 SEM pictures at different magnifications taken from the fracture surface of EP/PESU-L (10 wt %).

RESULTS AND DISCUSSIONS

Phase structure

The DSC traces show a T_g step at $T \approx 150$–190°C (Fig. 1) which is followed by a second step superimposed to a small exothermic peak representing postcuring. Note that this exothermic peak is overlapping with the region of glass transition of PESU (at $T_g \approx 220$°C cf. Table I). One can also see that the MM of the PESU used did not affect significantly the T_g of the modified resins. The DSC T_g data are summarized in Table II. The reduction in T_g is due to two major reasons: (i) offset stoichiometry caused by the reaction between —OH(PESU) and anhydride(MTHPA hardener), and (ii) hampered crosslinking of the EP owing the PESU incorporation induced viscosity increase.

DMTA curves depicting the storage modulus (E') and mechanical loss factor (tan δ) as a function of temperature (T) for the EP, and EP/PESU systems with 10 wt % PESU of various MM are shown in Figure 2. Note that the storage modulus of EP in the glassy state does not change by adding PESU and the MM of the latter has also a negligible influence on the stiffness. This is because the T_g of PESU is higher than that of the EP. The peaks at $T \approx -70$°C and 170°C, respectively, show the beta and alpha(T_g)-relaxations of the EP resin, respectively. Note that in line with DSC results, a reduction in the T_g values can be observed for the PESU-modified EPs compared with the reference EP. The T_g values, read as the temperature of the maximum of the α-relaxation in the DMTA spectra, are listed also in Table II. The T_g data in Table II substantiate that the T_g of EP does not change significantly with the MM of PESU. The results obtained from DMTA measurements are in good agreement with the DSC T_g data. T_g of PESU could not be resolved in the DMTA traces because of its overlapping with that of the parent EP.

It is well demonstrated in the literature that PESU is present as a separated phase in the EP. The two-phase structure was confirmed by SEM inspection. Figures 3–5 display SEM pictures taken from the fracture surfaces of the EP/PESU (10 wt %) systems containing PESU of different MM.

The morphology of the PESU-modified EP shows two striking features based on the SEM results. First, PESU-L and PESU-M are uniformly and finely dispersed (cf. Figs. 3 and 4). However, the mean particle size increases with increasing MM. The mean particle sizes of the spherical inclusions of PESU-L and PESU-M are in the ranges of 200–700 nm and 0.4–1.4 μm, respectively. The other peculiarity is that PESU-H is present in irregularly shaped domains

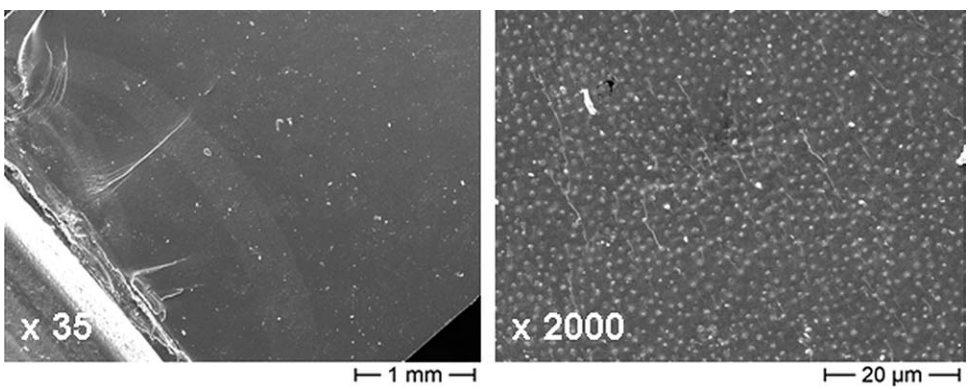

Figure 4 SEM pictures at different magnifications taken from the fracture surface of EP/PESU-M (10 wt %).

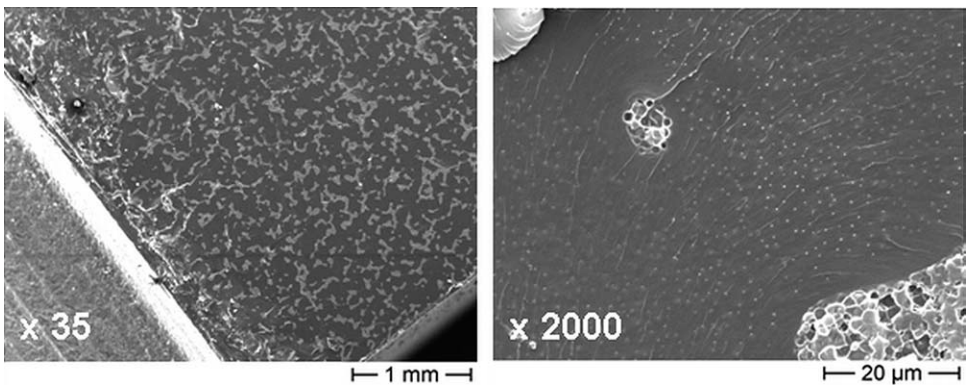

Figure 5 SEM pictures at different magnifications taken from the fracture surface of EP/PESU-H (10 wt %).

(cf. Fig. 5). A closer look in these domains reveals that they are formed by massive agglomeration of the initially developed spherical droplets (Fig. 6). In these domains, the primary PESU particles are hold together by an EP "binder" layer. The complex structure of such domains is usually termed to sea-island. It is noteworthy that the size range of the primary particles of PESU-H (300–800 nm) within the large, micron scale inclusions is similar to those of EP/PESU-L and EP/PESU-M. Based on experimental results, it has been suggested that the reaction-induced phase separation in EP/PESU systems takes place via spinodal decomposition mechanism.[22,28] Similar conclusion was deduced for EP/polyetherimide systems, as well.[43,44] However, this explanation is topic of dispute. Nonetheless, depending on the relative rates of the chemical reaction and the phase separation, different structures, such as isolated domains in uniform or bimodal distributions, or interconnected globules can be obtained.[45–47] It can be surmised that with increasing MM the compatibility between PESU and EP is reduced. Parallel to that the viscosity of EP/PESU increases with increasing MM of PESU at a given PESU concentration. These two parameters, which affect the reaction-induced phase separation processes, are responsible for the difference in the final morphologies observed for the EP/PESU systems.

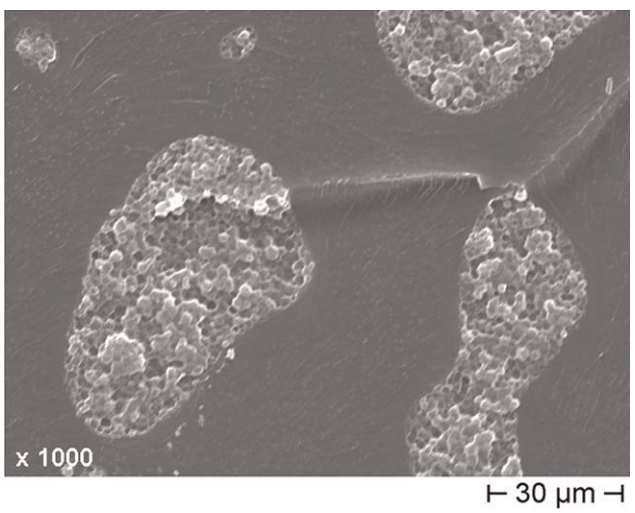

Figure 6 High magnification SEM picture showing the sea-island structure of the PESU phase on the fracture surface of EP/PESU-H (10 wt %).

Fracture mechanics

The K_c and G_c data are also included in Table II. One can see that with increasing MM of PESU the fracture mechanical parameters were improved. However, notable improvement in fracture toughness ($\sim$ 40%) was only observed by the incorporation of PESU-H. Adding PESU-M and PESU-L did not influence the K_c. On the other hand, G_c increased with increasing MM of PESU. The fact that K_c only slightly, whereas G_c markedly changed with PESU incorporation can be explained by changes in the load—load line displacement curves measured on the CT specimens. The maximum load, where fracture starts, does not change much by PESU modification. On the other hand, PESU incorporation causes crack tip blunting associated with increased displacement. As a consequence, the energy absorbed (surface below the load–load line displacement curve, which is linked with G_c) increases. Evidence for crack tip blunting is the appearance of the so called "plastic zone" that can be detected on the fracture surfaces of the specimens by SEM (cf. left-handed SEM pictures in Figs. 3–5). The improvements in G_c, caused by PESU-L and PESU-M, are comparable ($\sim$ 20% enhancement), and far less than achieved by PESU-H ($\sim$ 140%). Its reason is of morphological origin. The above described differences in the structures of EP/PESU in function of MM of PESU should result in different failure modes as disclosed next.

Failure mode

The failure mode of EP/PESU changes in function of PESU type. The finely dispersed spherical PESU

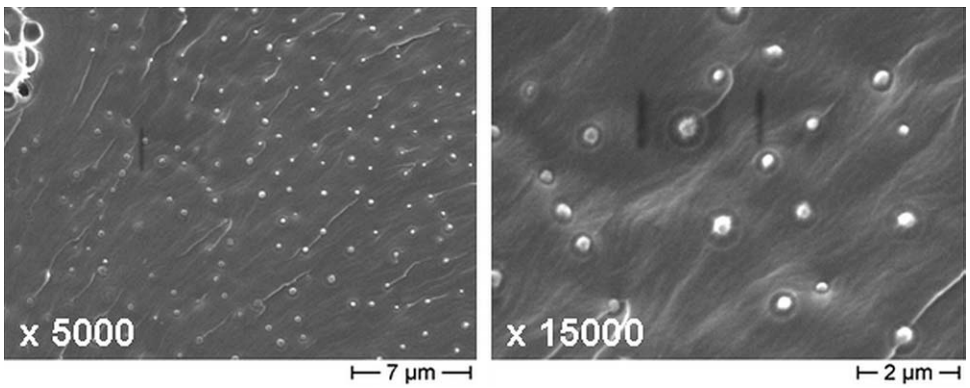

Figure 7 SEM pictures at different magnifications taken from the fracture surface of EP/PESU-H (10 wt %).

particles act as obstacles and cause crack pinning. The latter is well confirmed by the "tails" which are formed when the bowed crack front reunifies just passing the PESU droplet (obstacle). Crack pinning is, however, accompanied with shear rib formation in the EP matrix (cf. Fig. 7). The shear deformation is strongly supported by the fine dispersion of PESU along with a small distance (ligament) between the spherical particles.

The major reason of the finding that K_c and G_c increase with increasing MM (cf. data in Table II) is due the characteristics of the dispersed PESU phase. Irregularly shaped large PESU inclusions in EP contribute to "blunting" the crack in the notch root before final fast fracture takes place. This blunting occurs by crack bifurcation as evidenced in the SEM pictures in Figure 8. The bifurcation generated "process zone" at the notch is well perceptible in the SEM pictures in Figure 8. Be aware that the onset of a process zone is always a clear indication for toughness improvement in brittle thermosets.[48]

Thermostability

As it is shown in Figure 9, the onset of thermal degradation of PESU-modified EPs is slightly reduced. This appears especially clear for the EP/PESU-L combination. This suggests that thermal stability of neat EP is higher than that of the PESU grades used. This behavior may also be linked with the possible deviation from stoichiometry due to reaction of EP and hardener with the OH-groups of PESU, as well as with the differences observed in the morphologies of the EP/PESU systems. The values of temperature linked with 5 wt % mass loss are also presented in Table II. In the first approximation, one can claim that the reduction in the onset of the thermal degradation (i.e., $T_{5\%}$) is the smaller the higher the MM of the PESU modifier is (the ranking according to the corresponding data in Table II is as follows: PESU-L $<$ PESU-H $<$ PESU-M). This may be a hint that the off-stoichiometry is the key factor in this respect. Attention should be called to the fact that PESU incorporation is associated with an increase of the char yield. The related data, read as the residual mass at $T = 600°C$, are also listed in Table II.

CONCLUSIONS

This work was devoted to study the effect of molecular mass (MM) of hydroxyl terminated polyethersulfone (PESU) grades on the structure and fracture

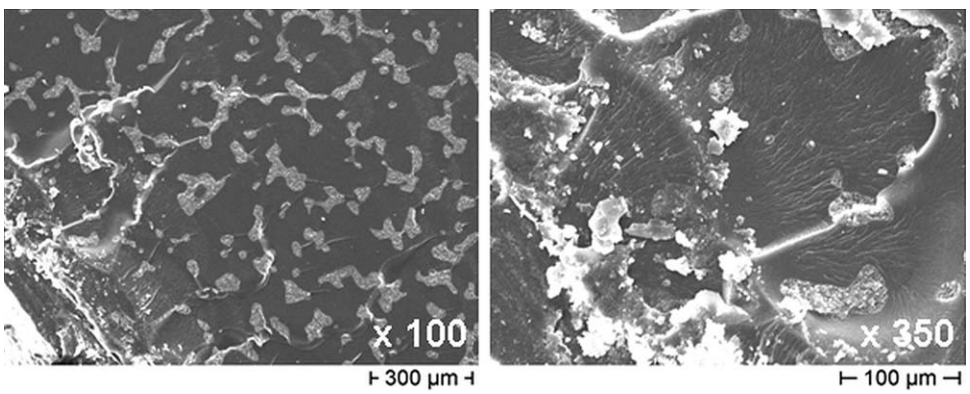

Figure 8 SEM pictures at different magnifications taken from the fracture surface at the initial notch of EP/PESU-H (10 wt %).

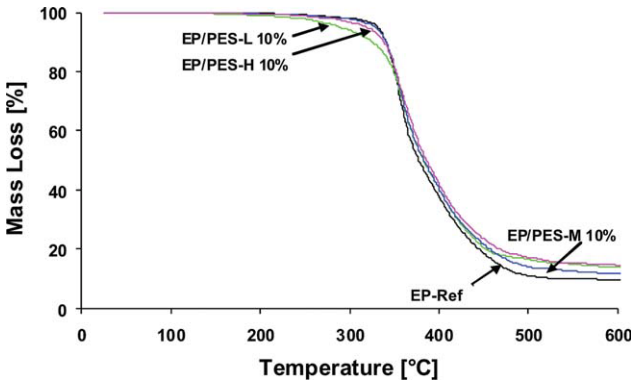

Figure 9 TGA curves for EP and EP/PESU (10 wt %) containing PESU of low (L), medium (M), and high (H) MM. [Color figure can be viewed in the online issue, which is available at wileyonlinelibrary.com.]

properties of an anhydride hardened tetrafunctional epoxy (EP) resin. The MM of the PESU grades, added in 10 wt %, were between 16 and 39 kDA in respect to their M_w values. The results received can be summarized as follows:

Morphology

The dispersion of the phase-separated PESU depended on its MM. PESU of low and medium MM were dispersed in the EP matrix in submicron scale spherical droplets uniformly. By contrast, PESU of high MM was present in large micron scale domains of sea-island structure. The size of the primary particles within the large domains (i.e., islands) was, however, comparable with those of PESU with low and medium MM.

Thermal properties

PESU incorporation slightly reduced the T_g. This was traced to off-stoichiometry caused by the possible reactions between the —OH groups of PESU and anhydride and EP during dissolution and curing, and sterical hindrance generated by the viscosity increase owing to the dissolved PESU. The onset of thermal degradation was slightly reduced by PESU incorporation, whereas an adverse trend was found in respect to the char yield.

Fracture and failure properties

The fracture toughness (K_c), and especially the fracture energy (G_c), were improved with enhanced MM of PESU. The related improvement depended on the dispersion of the PESU phase. Finely and homogeneously dispersed submicron scale spherical droplets of PESU of low and medium MM triggered crack pinning accompanied with slight improvements in K_c and G_c. On the other hand, the large micro scale domains of PESU of high MM supported crack bifurcation associated with shear rib formation of the EP matrix. The outcome was markedly enhanced K_c and G_c data compared with the EP reference and EP/PESU systems with PESU grades of low and medium MM.

References

1. Ritzenthaler, S.; Girard-Reydet, E.; Pascault, J. P. Polymer 2000, 41, 6375.
2. Kim, S. T.; Kim, J.; Lim, S.; Choe, C. R.; Hong, S. I. J Mater Sci 1998, 33, 2421.
3. Nichols, M. E.; Robertson, R. E. J Mater Sci 1994, 29, 5916.
4. Chen, S.-C.; Chiu, H.-T.; Ye, C.-P. J Appl Polym Sci 2002, 86, 3740.
5. Vanden Poel, G.; Goossens, S.; Goderis, B.; Groeninckx, G. Polymer 2005, 46, 10758.
6. Goossens, S.; Goderis, B.; Groeninckx, G. Macromolecules 2006, 39, 2953.
7. Kim, J. K.; Robertson, R. E. J Mater Sci 1992, 27, 161.
8. López, J.; Ramírez, C.; Abad, M. J.; Barral, L.; Cano, J.; Díez, F. Polym Int 2002, 51, 1100.
9. Teng, K.-C.; Chang, F.-C. Polymer 1996, 37, 2385.
10. Francis, B.; Rao, V. L.; Ramaswamy, R.; Jose, S.; Thomas, S.; Raju, K. V. S. N. Polym Eng Sci 2005, 45, 1645.
11. Zhang, X.-J.; Yi, X.-S.; Xu, Y.-Z. J Appl Polym Sci 2008, 109, 2195.
12. Bonnaud, L.; Pascault, J. P.; Sautereau, H. Eur Polym Mater 2000, 36, 1313.
13. Gan, W.; Yu, Y.; Wang, M.; Tao, Q.; Li, S. Macromol Rapid Commun 2003, 24, 952.
14. Wang, M.; Yu, Y.; Wu, X.; Li, S. Polymer 2004, 45, 1253.
15. Gianotti, M. I.; Mondragon, I.; Galante, M. J.; Oyanguren, P. A. Polym Int 2005, 54, 897.
16. Varley, R. Macromol Mater Eng 2007, 292, 46.
17. Min, H. S.; Kim, S. C. Polym Bull 1999, 42, 221.
18. Van Overbeke, E.; Carlier, V.; Devaux, J.; Carter, J. T.; McGrail, P. T.; Legras, R. Polymer 2000, 41, 8241.
19. Chen, C.-C.; Chen, Y.-S.; Shen, K.-S.; Yu, T. L. J Polym Res 2003, 10, 39.
20. Cedeño, A. J.; Vázquez-Torres, H. Polym Int 2005, 54, 1141.
21. Kim, B. S.; Inoue, T. Polymer 1995, 36, 1985.
22. Andrés, M. A.; Garmendia, J.; Valea, A.; Eceiza, A.; Mondragon, I. J Appl Polym Sci 1998, 69, 183.
23. Hodgkin, J. H.; Simon, G. P.; Varley, R. J Polym Adv Technol 1998, 9, 3.
24. Fernández, B.; Corcuera, M. A.; Marieta, C.; Mondragon, I. Eur Polym Mater 2001, 37, 1863.
25. Mimura, K.; Ito, H. J Appl Polym Sci 2003, 89, 527.
26. Carter, J. T.; Emmerson, G. T.; Lo Faro, C.; McGrail, P. T.; Moore, D. R. Compos A 2003, 80, 83.
27. Fernández, B.; Arbelaiz, A.; Diaz, E.; Mondragon, I. Polym Compos 2004, 25, 480.
28. Blanco, I.; Cicala, G.; Motta, O.; Recca, A. J Appl Polym Sci 2004, 94, 361.
29. Tang, X.; Zhang, L.; Wang, T.; Yu, Y.; Gan, W.; Li, S. Macromol Rapid Commun 2004, 25, 1419.
30. Park, S.-J.; Li, K.; Jin, F.-L. J Ind Eng Chem 2005, 11, 720.
31. Jin, F.-L.; Park, S.-J. Polym Degr Stab 2007, 92, 509.
32. Gan, W.; Zhan, G.; Wang, M.; Yu, Y.; Xu, Y.; Li, S. Colloid Polym Sci 2007, 285, 1727.
33. Zhao, L.; Zhan, G.; Yu, Y.; Tang, X.; Li, S. J Appl Polym Sci 2008, 108, 953.
34. Zhang, J.; Guo, Q.; Fox, B. J Appl Polym Sci 2009, 113, 485.
35. Man, Z.; Stanford, J. L.; Dutta, B. K. J Appl Polym Sci 2009, 112, 2391.

36. Quipeng, G. Polymer 1993, 34, 70.
37. Kishi, H.; Shi, Y.-B.; Huang, J.; Yee, A. F. J Mater Sci 1997, 32, 761.
38. Mimura, K.; Ito, H.; Fujioka, H. Polymer 2000, 41, 4451.
39. Bonnaud, A.; Bonnet, J. P.; Pascault, H.; Sautereau, C. C.; Riccardi, L. J Appl Polym Sci 2002, 83, 1385.
40. Bucknall, C. B.; Partridge, I. K. Br Polym J 2006, 15, 71.
41. Peng, M.; Li, H.; Wu, L.; Chen, Y.; Zheng, Q.; Gu, W. Polymer 2005, 46, 7612.
42. Asif, A. A.; John, B.; Rao, V. L.; Ninan, K. N. Polym Int 2010, 59, 986.
43. Bucknall, C. B.; Partridge, I. K. Polymer 1983, 24, 639.
44. Bucknall, C. B.; Gomez, C. M.; Quintard, I. Polymer 1994, 35, 353.
45. Inoue, T. Prog Polym Sci 1995, 20, 119.
46. Hwang, J. W.; Cho, K.; Yoon, T. H.; Park, C. E. J Appl Polym Sci 2000, 77, 921.
47. Riew, C., Kinloch, A. J., Eds. Toughened Plastics, I, In Advances in Chemistry Series 233; American Chemical Society: Washington, DC, 1993.
48. Karger-Kocsis, J. In Nano- and Micromechanics of Polymer Blends and Composites; Karger-Kocsis, J.; Fakirov, S., Eds.; Hanser: Munich, 2009; Chapter 12, pp. 425–470.